Neuron, Vol. 31, 957–971, September 27, 2001, Copyright ©2001 by Cell Press

Necrotic Cell Death in *C. elegans* Requires the Function of Calreticulin and Regulators of Ca^{2+} Release from the Endoplasmic Reticulum

Keli Xu, Nektarios Tavernarakis,[2] and Monica Driscoll[1]
Department of Molecular Biology and Biochemistry
Rutgers, The State University of New Jersey
A232, Nelson Biological Laboratories
604 Allison Road
Piscataway, New Jersey 08855

Summary

In *C. elegans*, a hyperactivated MEC-4(d) ion channel induces necrotic-like neuronal death that is distinct from apoptosis. We report that null mutations in calreticulin suppress both *mec-4(d)*-induced cell death and the necrotic cell death induced by expression of a constitutively activated $G\alpha_s$ subunit. RNAi-mediated knockdown of calnexin, mutations in the ER Ca^{2+} release channels *unc-68* (ryanodine receptor) or *itr-1* (inositol 1,4,5 triphosphate receptor), and pharmacological manipulations that block ER Ca^{2+} release also suppress death. Conversely, thapsigargin-induced ER Ca^{2+} release can restore *mec-4(d)*-induced cell death when calreticulin is absent. We conclude that high $[Ca^{2+}]_i$ is a requirement for necrosis in *C. elegans* and suggest that an essential step in the death mechanism is release of ER-based Ca^{2+} stores. ER-driven Ca^{2+} release has previously been implicated in mammalian necrosis, suggesting necrotic death mechanisms may be conserved.

Introduction

Cell death plays critical roles in both development and pathological conditions. Influential work that helped lay the foundation of the cell death field originally distinguished two types of cell death on morphological grounds (Kerr et al., 1972). Apoptosis is a mode of cell death common in development and homeostasis that occurs by a biochemical program conserved from nematodes to humans (Metzstein et al., 1998). Necrosis, characterized by swelling of the dying cell, generally occurs under conditions of cellular injury. Despite the profound effects of necrotic cell death consequent to stroke, ischemia, and various neurodegenerative conditions, molecular mechanisms of necrosis remain poorly understood (Martin et al., 1998).

In *C. elegans,* necrotic-like cell death can be induced by several genetically delivered insults, including gain-of-function mutations in degenerin ion channel genes (Chalfie and Wolinsky, 1990; Driscoll and Chalfie, 1991), a dominant mutation specifying a nondesensitizing acetylcholine receptor channel (Treinin and Chalfie, 1995) and expression of constitutively activated $G\alpha_s$ (Korswagen et al., 1997; Berger et al., 1998). One of the best-studied necrosis initiators in the nematode is the mutant degenerin Na^+ channel MEC-4(d), which induces neurodegeneration via a mechanism reminiscent of that operative in mammalian excitotoxic cell death—the hyperactivation of ion channels. Large side chain amino acid substitutions near the MEC-4 channel pore (encoded by dominant *mec-4(d)* alleles) are thought to favor an open-channel conformation, causing excess ion influx that is ultimately toxic (Hong and Driscoll, 1994; Adams et al., 1998). Analogous substitutions in related mammalian DEG/ENaC channels can cause cell swelling and degeneration (Waldmann et al., 1996).

At the ultrastructural level, the dying neuron expressing the MEC-4(d) channel first produces electron dense membraneous whorls near the plasma membrane that appear to coalesce into larger cellular inclusions (Hall et al., 1997). Later, the nucleus becomes distorted, chromatin clumps, and organelles swell and degrade. Ultimately, cytoplasm and organelles disappear and the cell corpse, which is usually still surrounded by a plasma membrane, is removed by a process that requires programmed cell death phagocytosis genes (Chung et al., 2000). *mec-4(d)*-induced death occurs independently of *C. elegans* apoptosis regulators and executors (*egl-1, ced-9, ced-4*, and *ced-3)* and thus is genetically distinct from programmed cell death (Chung et al., 2000). At present, categorization of *mec-4(d)*-induced cell death is difficult since certain morphological features of *mec-4(d)*-induced death are shared with classic necrosis, with type 3B developmental cell death, and with autophagy (death types described by Clarke, 1990). The presence of prominent intracellular inclusions in *mec-4(d)*-induced cell death also suggests that the aggregation toxicity that characterizes several human neurodegenerative disorders (Hardy and Gwinn-Hardy, 1998) could be operative. Because *mec-4(d)*-induced cell death is well documented to be induced by ion channel hyperactivation and is associated with cell swelling, we refer to it as a necrotic type of cell death.

To gain insight into the molecular mechanisms of necrotic cell death in *C. elegans*, we conducted a genetic screen for suppressors of *mec-4(d)*-induced cell death. We identified eight loci that can mutate to block effects of *mec-4(d)* expressed ectopically in the ventral nerve cord. Mutations affecting one suppressor locus protected against necrosis induced by channel-hyperactivating degenerin subunits encoded by *mec-4(d)* and *deg-1(d)* as well as against necrotic cell death induced by activated $G\alpha_s$. We found that this locus encodes calreticulin (*crt-1)*, a Ca^{2+} binding/storing protein found primarily in the lumen of the endoplasmic reticulum (ER) that serves both as a molecular chaperone and as a central regulator of Ca^{2+} homeostasis (reviewed in Michalak et al., 1999; Llewellyn et al., 2000). We found that three additional genes involved in ER regulation of intracellular Ca^{2+}—the ER calcium binding chaperone calnexin homolog *cnx-1*, the ER Ca^{2+} release channel inositol triphosphate receptor channel InsP3R, *itr-1* (Dal Santo et al., 1999), and the ER Ca^{2+} release channel

[1] Correspondence: driscoll@mbcl.rutgers.edu
[2] Present address: Institute of Molecular Biology and Biotechnology, Foundation for Research and Technology, Vassilika Vouton, P.O. Box 1527, GR 711 10 Heraklion, Crete, Greece.

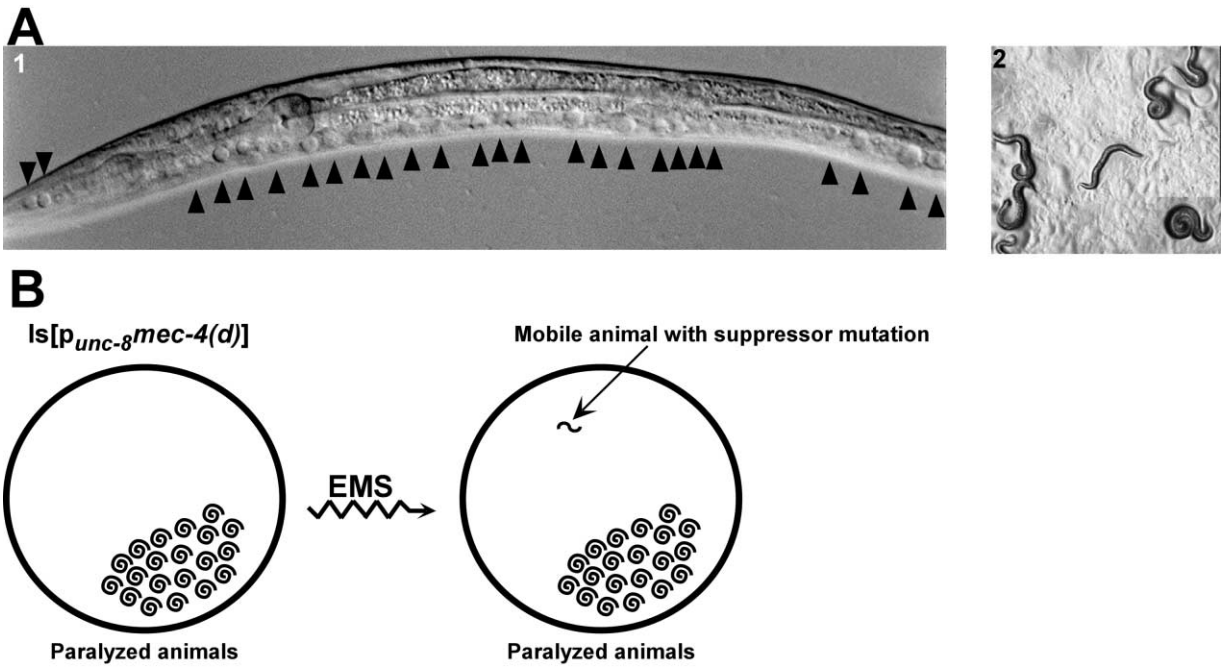

Figure 1. An Efficient Screen for Suppressors of Neurodegeneration Induced by Ectopic Expression of *mec-4(d)*

(A) Strain ZB194 (*bz32* Is[p_{unc-8}*mec-4(d)*]), which harbors an integrated array of plasmid p_{unc-8}*mec-4(d)*, exhibits swelling and degeneration of many ventral cord neurons as well as some head and tail neurons. Arrows indicate dying cells detectable in the focal plane (panel 1). Is[p_{unc-8}*mec-4(d)*] mutants are uncoordinated and severely paralyzed. Note the coiling and absence of tracks in the *E. coli* lawn in a typical photo taken 2 hr after animals were placed onto a plate (panel 2).

(B) Strategy for isolation of suppressors of *mec-4(d)*-induced degeneration. Is[p_{unc-8}*mec-4(d)*] animals are severely paralyzed due to motor neuron degeneration. After EMS mutagenesis, F2 progeny that exhibit restored locomotion are candidate suppressor mutants in which the deleterious effects of *mec-4(d)* are blocked.

ryanodine receptor channel RyR *unc-68* (Maryon et al., 1996)—must function for efficient *mec-4(d)*-induced cell death. Our data support a model in which regulation of, and possibly release of, ER Ca^{2+} stores is a requirement for neurotoxicity of hyperactivated ion channels in *C. elegans.* Given well-known but still poorly understood contributions of Ca^{2+} to necrotic cell death in higher organisms (reviewed in Lee et al., 1999; Mattson et al., 2000; Sattler and Tymianski, 2000), our data provide the first indication that mechanisms underlying necrotic cell death may be conserved from nematodes to humans. In highlighting four specific death suppressor loci involved with ER-based Ca^{2+} release/homeostasis, this work underscores the importance of the contribution of ER-based intracellular Ca^{2+} storage/release to channel injury–induced neuropathology.

Results

Single Gene Mutations Can Block Necrotic-like Cell Death in *C. elegans*

The MEC-4(d) channel acts cell autonomously to induce necrotic death of specific cells when expressed ectopically in *C. elegans* (Harbinder et al., 1997). In particular, we previously noted that transgene expression of *mec-4(d)* in the ventral nerve cord causes a significant reduction in numbers of DAPI-stained nuclei in the cord (Harbinder et al., 1997). To identify genes required for necrotic-like neuronal cell death, we ectopically expressed *mec-4(d)* in the *C. elegans* ventral nerve cord under the control of the *unc-8* promoter (Tavernarakis et al., 1997). In nematodes harboring an integrated array of p_{unc-8}*mec-4(d)* (strain designated Is[p_{unc-8}*mec-4(d)*]), many neurons in the ventral cord, as well as some neurons in the head and tail ganglia, swell and degenerate. Is[p_{unc-8}*mec-4(d)*] animals are consequently severely paralyzed (Figure 1A, Table 1A).

We took advantage of the paralyzed phenotype to screen for suppressor mutations that block the deleterious effects of *mec-4(d)* by mutagenizing Is[p_{unc-8}*mec-4(d)*] and identifying rare animals in which nearly wild-type locomotion was restored (Figure 1B). In a screen of 45,000 haploid mutagenized Is[p_{unc-8}*mec-4(d)*] genomes, we isolated 24 strong suppressor mutations. All the suppressed strains retain the integrated p_{unc-8}*mec-4(d)* array (see Experimental Procedures) and thus suppressor mutations counter the deleterious effects of the Is[p_{unc-8}*mec-4(d)*] array rather than disrupt the toxic transgene. Four recessive suppressor alleles, *bz29*, *bz30*, *bz31*, and *bz50*, map to chromosome V and fail to complement each other, suggesting that they identify a single locus. For the sake of clarity in nomenclature, we note here that we identified this gene as *crt-1*, which encodes calreticulin (see below).

Strong *crt-1* Alleles Suppress Cell Death Induced by Is[p_{unc-8}*mec-4(d)*]

We first examined *crt-1;* Is[p_{unc-8}*mec-4(d)*] suppressor mutants for the presence of degenerating neurons using Nomarski DIC optics microscopy (Table 1A). We found that both the number and the size of swollen neuronal

Table 1. Phenotypic Characterization of *crt-1* Mutants

	crt-1(+)	*crt-1(bz29)*	*crt-1(bz30)*	*crt-1(bz31)*	*crt-1(bz50)*
A. Suppression Of Toxic Effects Induced by Is[p_{unc-8}*mec-4(d)*]					
Is[p_{unc-8}*mec-4(d)*] (paralysis[a])	100	0	0	0	0
Is[p_{unc-8}*mec-4(d)*] (swollen cell bodies[b])	82 ± 9	9 ± 4	11 ± 3	38 ± 6	54 ± 8
B. Suppression of Toxic Effects Induced by Other Genetic Insults					
mec-4(u231) (swollen touch cell bodies[c])	95 ± 1	3 ± 2	3 ± 2	95 ± 2	82 ± 4
bzIs3 (swollen touch cell bodies[d])	95 ± 2	5 ± 2	ND	ND	ND
mec-4(u231) (MEC-4::GFP[e])	4 ± 3	84 ± 7	ND	ND	ND
deg-1(u38) (swollen neuronal cell bodies[f])	86 ± 7	13 ± 11	ND	ND	ND
unc-8(n491) (inability to backup[g])	100	0	0	100	100
unc-105(n1274) (paralysis[h])	100	0	ND	100	100
nuIs5 $p_{glr-1}G\alpha_s(gf)$ (PVC cell death[i])	87 ± 4	39 ± 5	ND	ND	ND
deg-3(u662) (swollen cell bodies[j])	5.1 ± 0.4	5.7 ± 0.6	5.8 ± 0.4	5.5 ± 0.7	ND
C. Phenotypes of *crt-1* Mutants					
Generation time (h)[k]	71.1 ± 1.3	97.0 ± 1.9	94.0 ± 1.5	68.3 ± 1.1	73.2 ± 1.8
Body length (mm)[l]	1.2 ± 0.1	0.7 ± 0.2	0.8 ± 0.1	1.1 ± 0.1	1.3 ± 0.2
Brood size[m]	198 ± 145	215 ± 17	206 ± 14	211 ± 16	213 ± 14
Defecation period (sec)[n]	46.7 ± 3	51.1 ± 4	52.2 ± 4	49.1 ± 5	50.8 ± 4
Touch sensitivity[o]	93 ± 4	82 ± 4	79 ± 5	86 ± 6	83 ± 4
Sensitivity to sustained touch	89 ± 6	21 ± 8	30 ± 6	78 ± 7	69 ± 5

[a] Paralysis was assayed by placing mutants on plates and scoring migration from site of origin after 2 hr. Score indicates percentage of mutants migrating less than 1 cm in 2 hr (n = 50).

[b] Swollen cell bodies in the ventral nerve cord (between the posterior end of the pharynx and anterior of the tail ganglia) were counted in Is[p_{unc-8}*mec-4(d)*] and *crt-1*; Is[p_{unc-8}*mec-4(d)*] animals at the L1 stage. Score indicates % animals having more than five detectable swollen cells in the ventral cord (n > 95). When present, swellings in the *crt-1*; Is[p_{unc-8}*mec-4(d)*] background are uniformly small and difficult to detect as compared to the Is[p_{unc-8}*mec-4(d)*] strain.

[c] Percentage of L1 larvae that exhibit degeneration of PLM touch receptor neurons, cells which normally express *mec-4*, is indicated (n > 100).

[d] Percentage of L1 larvae that exhibit degeneration of PLM touch receptor neurons; *bzIs3* is an integrated transgene array that includes 10× the normal gene dosage of *mec-4(d)* and causes accelerated degeneration (Hall et al., 1997) (n > 100).

[e] Percentage of adults with PLM touch cell fluorescence consequent to the introduction of a p_{mec-4}MEC-4::GFP transgene (n > 100).

[f] Percentage of L1 mutants that exhibit degenerating cells in the head (positive score is 3 or more evident vacuoles; n > 129).

[g] Percentage of mutants that fail to move backward normally in response to head touch is indicated (n > 100).

[h] Percentage of mutants that fail to migrate more than 1 cm from the site they were placed after 2 hr is indicated (n = 50).

[i] Percentage of adults missing at least one (of two easily distinguished) fluorescent PVC neuron (n > 110). *nuIs5* includes a p_{glr-1}GFP fusion gene used to visualize cells in which the *glr-1* promoter is active (Berger et al., 1998).

[j] Scores are average number of degenerating cells per L1 stage animal (n > 124).

[k] Generation time, defined as time from first egg deposition to next generation egg deposition, was assayed at 20°C, approximately 20 animals each strain scored, 2 trials.

[l] Body length is the average measurement of 20 L4 animals.

[m] Brood size is the average brood of 20 hermaphrodites; in all cases, 95% or more of embryos hatch.

[n] Defecation period is the average number of seconds between expulsions (n = 10 animals over 10 cycles for each strain).

[o] For touch sensitivity (response to initial touches) and sustained touch sensitivity (response to consecutive touches), % responding of 100 is indicated.

somata are dramatically decreased in *crt-1;* Is[p_{unc-8}*mec-4(d)*] L1 larvae. For example, 82% of animals of parental genotype Is[p_{unc-8}*mec-4(d)*] had more than five prominent swellings in the ventral nerve cord, whereas only 9% of *crt-1(bz29);* Is[p_{unc-8}*mec-4(d)*] mutants exhibited a similar extent of ventral cord swellings, and swollen cell bodies in the *crt-1* backgrounds were always significantly smaller than those in the parental line. Interestingly, alleles *crt-1(bz31)* and *crt-1(bz50)* are weaker suppressors of cell swelling than are *crt-1(bz29)* and *crt-1(bz30),* yet locomotion of all the suppressed lines is comparable and appears grossly normal. This indicates that motorneurons can still function even when a modest swelling of neuronal cell bodies occurs.

crt-1 Mutations Can Suppress Effects of Hyperactive Degenerin Channels Expressed in Neurons and Muscles

To rule out that *crt-1* mutations specifically block toxicity of ectopically expressed *mec-4(d)* by silencing of transgene expression, we tested their abilities to suppress touch receptor necrosis induced by *mec-4(d)* allele *u231*, which encodes the hyperactivating MEC-4(A713V) channel subunit (Driscoll and Chalfie, 1991; Hong and Driscoll, 1994). We constructed *crt-1; mec-4(d)* double mutants and scored swollen touch cells at the L1 larval stage (Table 1B). We found that both *crt-1(bz29)* and *crt-1(bz30)* efficiently suppress *mec-4(d)*-induced touch cell degeneration (95% degeneration in *mec-4(d)* mutants but only 3% degeneration in *crt-1(bz29* or *bz30); mec-4(d)*). *crt-1(bz29)* is also a highly efficient suppressor of touch cell necrosis caused by *bzIs3*, an integrated transgene array in which the *mec-4(d)* gene is present at approximately 10× the normal gene dosage (Table 1B). Cell death occurs with an accelerated time course in this strain, presumably because of an increased cellular insult (Hall et al., 1997).

As indicated by previous characterization of *mec-4(d)*-induced death (Hall et al., 1997), neuronal swelling in the touch neurons is strongly correlated with cell elimi-

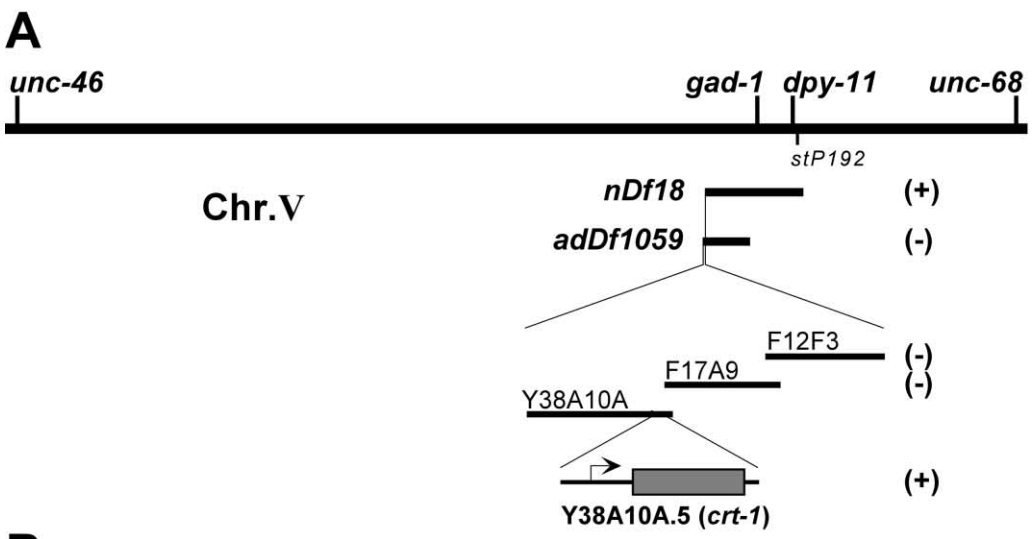
A
unc-46
gad-1
dpy-11
unc-68
stP192
Chr.V
nDf18
(+)
adDf1059
(-)
F12F3
(-)
F17A9
(-)
Y38A10A
(+)
Y38A10A.5 (crt-1)

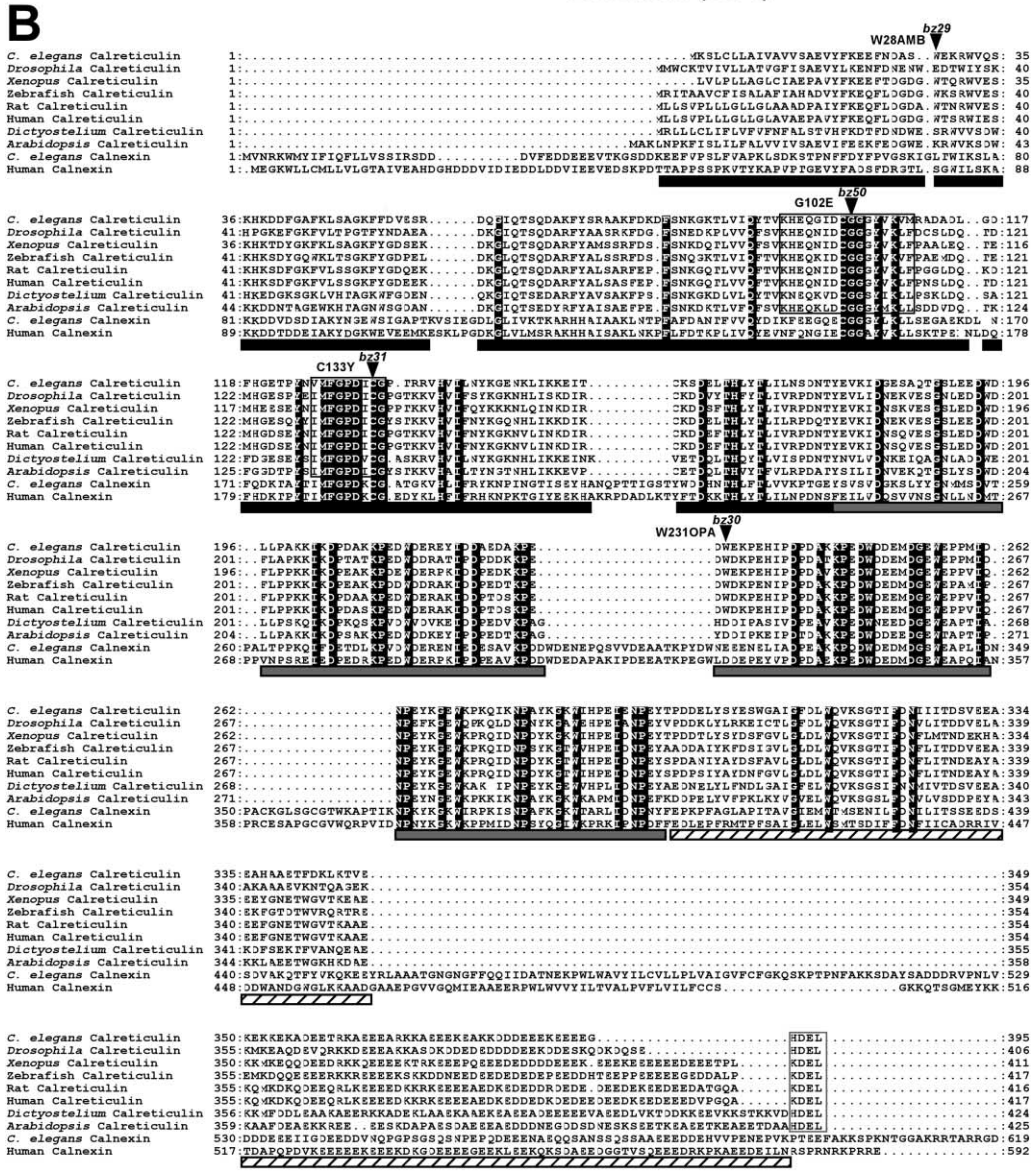
B
W28AMB
bz29
G102E
bz50
C133Y
bz31
W231OPA
bz30
C. elegans Calreticulin
Drosophila Calreticulin
Xenopus Calreticulin
Zebrafish Calreticulin
Rat Calreticulin
Human Calreticulin
Dictyostelium Calreticulin
Arabidopsis Calreticulin
C. elegans Calnexin
Human Calnexin

nation. When we introduced a p_{mec-4}MEC-4::GFP reporter on an extrachromosomal array to facilitate visualization of living touch receptor neurons, we found that only 4% of *mec-4(d)* mutants have at least one viable fluorescing PLM cell whereas 84% of *crt-1(bz29); mec-4(d)* animals exhibited at least one fluorescent PLM neuron (Table 1B). We conclude that suppression is not restricted to modulation of cell swelling, but rather affects neuronal viability itself. Moreover, these experiments establish that suppressor effects are not limited to toxic genes expressed from transgenic arrays nor are the effects of the suppressor mutations restricted to rescue of a single neuronal type. Unexpectedly, however, we found that *crt-1(bz31)* and *crt-1(bz50)* did not effectively suppress *mec-4(d)*-induced touch cell degeneration, indicating that *bz31* and *bz50* define a distinct class of alleles from *bz29* and *bz30*.

We next tested whether *crt-1* alleles could suppress dominant channel-hyperactivating mutations affecting other members of the *C. elegans* degenerin family (Table 1B). The dominant *deg-1(d)* allele *u38* specifies a toxic large side chain amino acid substitution at the position corresponding to the MEC-4(A713V) substitution, inducing swelling and neuronal death of several neurons that proceeds with an ultrastructural profile similar to *mec-4(d)*-induced death (Chalfie and Wolinsky, 1990; Garcia-Anoveros et al., 1995; Hall et al., 1997). Comparison of numbers of swollen neurons in the nerve rings of L1 stage animals revealed a significant suppression of *deg-1(d)* toxicity by *crt-1(bz29)*. Whereas 86% of *deg-1(d)* mutants had large swollen cells in the nerve ring, only 13% of *crt-1(bz29); deg-1(d)* mutants had detectable vacuoles at this stage, and most were smaller than in the *crt-1(+)* background (Table 1B). Thus, *crt-1(bz29)* can suppress toxicity conferred by multiple death-inducing degenerin mutations expressed in distinct groups of neurons.

Specific alleles of two other degenerins, *unc-8* and *unc-105,* affect amino acid residues at sites different from that corresponding to MEC-4(A713V), but can cause some degree of channel hyperactivation (Garcia-Anoveros et al., 1995; Tavernarakis et al., 1997). The *unc-8* degenerin channel is expressed in many ventral cord neurons (Tavernarakis et al., 1997) and gain-of-function allele *unc-8(n491)* has been previously noted to induce neuronal swelling (Shreffler et al., 1995). We have found that UNC-8::GFP expression disappears from many ventral cord neurons in the *unc-8(n491)* background and that numbers of DAPI-stained nuclei in this background are also reduced, suggesting that some ventral cord neurons die in this background (data not shown). *crt-1(bz29)* and *crt-1(bz30)* completely suppressed the severely uncoordinated phenotype of *unc-8(n491)*, which coils and cannot back up in response to touch on the head (Table 1B). Likewise, *crt-1(bz29)* fully suppressed the paralysis phenotype conferred by a gain-of-function allele of *unc-105(n1274)*, a degenerin that affects muscle but does not cause cell death (Liu et al., 1996; Garcia-Anoveros et al., 1998). We conclude that *crt-1* suppressor activity is not restricted to the *mec-4(d)* channel, and can be extended to different hyperactive degenerin channels expressed in neurons and muscles. We note, however, that neither *crt-1(bz31)* nor *crt-1(bz50)* could suppress *unc-8(n491)* or *unc-105 (n1274)*. Thus, *crt-1(bz31)* and *crt-1(bz50)* define a distinct class of *crt-1* alleles that can suppress neurotoxic effects of an ectopically expressed *mec-4(d)* channel, but fail to suppress deleterious effects of hyperactive degenerin channels expressed in their normal cellular contexts.

crt-1 Mutations Can Suppress Toxicity of Activated $G\alpha_s$ Expression

In *C. elegans*, expression of constitutively activated rat $G\alpha_s$[Q227L] induces necrotic-like death via a process that requires the *acy-1* adenylyl cyclase (Berger et al., 1998). To determine if *crt-1* alleles affect necrotic-like cell death induced by distinct initiating stimuli, we tested for effects on $G\alpha_s$-induced necrosis (Table 1B). We constructed *crt-1 nuIs5*[$p_{glr-1}G\alpha_s$ *(Q227L)* p_{glr-1}GFP] lines and quantitated survival of the easily scored PVC neurons by counting fluorescent cells (Table 1B). In the *nuIs5*[$p_{glr-1}G\alpha_s$ *(Q227L)* p_{glr-1}GFP] line, an average of 87% of animals had at least one (of two) fluorescent PVC neuron missing (Table 1B). By contrast, we find that only an average of 39% of *crt-1(bz29) nuIs5* animals lacked at least one PVC neuron. The *crt-1(bz29)* suppression of $G\alpha_s$-delivered insults demonstrates that the protective effects of *crt-1* mutations are not restricted to hyperactive degenerin channels. *crt-1* alleles can protect against necrotic-like cell death induced by distinct initiating insults.

crt-1 Mutations Do Not Protect against Necrosis Induced by Hyperactive Plasma Membrane Ca^{2+} Channel

Substitution I293N in TMDII of the plasma membrane acetylcholine receptor channel subunit DEG-3 alters channel desensitization, creating a channel with increased Ca^{2+} influx that induces necrotic-like cell death (Treinin and Chalfie, 1995; Treinin et al., 1998). To determine whether *crt-1* mutations block the deleterious effects of this hyperactivated Ca^{2+} channel, we constructed *crt-1; deg-3(d)* double mutants and scored for vacuolar swellings (Table 1B). We found no significant

Figure 2. The Death Suppressor Locus on Chromosome V Corresponds to *C. elegans* Calreticulin, *crt-1*

(A) Genetic and physical map of the region encompassing *crt-1*. Regions missing in deficiencies (Df) are indicated by bold lines; Yac (Y) and cosmid clones in the interval defined by the region of nonoverlap between *nDf18* and *adDf1059* are indicated by thin lines. In parentheses is indicated the ability of the deficiency, cosmid, or amplified open reading frame to complement *crt-1* mutations.

(B) Amino acid sequence alignment of calreticulin and calnexin proteins from representative organisms. The primary sequence of *crt-1* was predicted using the GENEFINDER algorithm (accession number P27798) and confirmed by the assembly of overlapping ESTs. Alignments were performed using the CLUSTALW algorithm. The N, P, and C domains are underlined by black, gray, and striped bars, respectively. The two calreticulin signature sites (Prosite) are boxed; the ER retrieval sequence is boxed in gray. Residues common to all calreticulin and calnexins are boxed in black. The identities of the amino acid changes in *crt-1* alleles *bz29*, *bz30*, *bz31*, and *bz50* are noted at positions indicated by arrows.

difference in the numbers of swollen cells at any stage. Thus, *crt-1* mutations appear unable to protect against neurotoxicity when elevated Ca^{2+} influx is delivered via a hyperactivated plasma membrane Ca^{2+} channel.

crt-1 Mutants Are Viable with Relatively Modest, but Pleiotrophic, Effects

To gain insight into the normal function of the *crt-1* locus, we examined the phenotypes of *crt-1* mutants in the absence of any toxic genes (Table 1C). We found that *bz29* and *bz30* developed more slowly than wild-type animals and were modestly shortened in body length. Brood sizes and embryo viability were normal in these backgrounds as assayed at 20°C (note that Park et al., 2001 report sterility at 25°C for a *crt-1* presumptive null deletion, a phenotype we confirmed for *crt-1(bz29)* and *crt-1(bz30)*, K.X., L. Herndon, and M.D., unpublished observations). *bz31* and *bz50* were neither slowed in development nor short in length. At least one rhythmic behavior, the defecation cycle, was normal in *crt-1* mutants.

Because the *mec-4* channel gene is normally expressed exclusively in the six touch receptor neurons and is required for their mechanosensory function, we carefully tested the response to gentle body touch in *crt-1* backgrounds. We found touch sensitivity is near normal in all four *crt-1* mutants, as conventionally scored by a few gentle strokes that alternate between head and tail (Chalfie and Sulston, 1981). However, we noticed that adaptation to continuous stimulation (the continued response to sustained stimuli alternating between head and tail touches; five or more consecutive touches) occurs more quickly in *crt-1(bz29)* and *crt-1(bz30)* backgrounds. The nearly normal touch sensitivity in the *crt-1* backgrounds suggests that suppressor mutations do not exert their effects by fully blocking biosynthesis and functional assembly of the MEC-4 channel in the touch neurons.

Degeneration Suppressors on Chromosome V Are Mutant Alleles of *C. elegans* Calreticulin, *crt-1*

Given the intriguing properties of our suppressor alleles, we sought to clone the locus defined by alleles *bz29*, *bz30*, *bz31*, and *bz50*. Using STS polymorphism mapping, three factor crosses, and deficiency mapping, we positioned the gene defined by these mutations very close to, but to the left of, *dpy-11* in the interval between the left endpoint of deficiency *adDf1059* and the left endpoint of deficiency *nDf18* (Figure 2A). To identify the gene, we attempted complementation rescue of the *bz29*; Is[p_{unc-8}*mec-4(d)*] strain by injecting cosmids harboring DNAs from the region. No cosmids mapping to the defined interval rescued the *bz29* mutant phenotype. We then systematically PCR amplified predicted genes housed only on YAC clones in the interval and tested their abilities to restore paralysis in the *bz29*; Is[p_{unc-8}*mec-4(d)*] background. Only one gene fragment, which included predicted open reading frame Y38A10A.5, caused transgenic animals to become severely paralyzed. We found that all four suppressor alleles were rescued by this fragment. Y38A10A.5 encodes the single *C. elegans* homolog of calreticulin (*crt-1*, 58% identity to human calreticulin), a Ca^{2+} binding protein primarily localized to the ER, which plays important roles in protein folding and maintenance of intracellular Ca^{2+} stores (Krause and Michalak, 1997; Michalak et al., 1999; Llewellyn et al., 2000). The *C. elegans crt-1* locus has been described at the molecular level (Smith, 1992), but mutations in this gene have not been previously identified. We identified mutations that affect the predicted exons of the *crt-1* gene in all four alleles (see Figure 2B), confirming that suppression of the Is[p_{unc-8}*mec-4(d)*] is a consequence of alterations in calreticulin function.

crt-1 alleles *bz29* (W28stop) and *bz30* (W231stop) both harbor nonsense mutations in the calreticulin coding region. The molecular identities of the mutations, together with the facts that (1) we have never been able to distinguish phenotypic differences between *bz29* and *bz30*, (2) mutants carrying the *bz29* or *bz30* mutations in trans to deficiency *adDf1059* have suppressor phenotypes indistinguishable from *bz29* and *bz30* homozygotes, (3) *bz29* and *bz30* exhibit growth and body size phenotypes indistinguishable from a *crt-1* deletion (Park et al., 2001), and (4) anti-CRT-1 immunoreactivity cannot be detected in *crt-1(bz29)* and *crt-1(bz30)* backgrounds (J. Ahnn, Kwangju Institute of Sci. and Tech., Korea, personal communication), suggest that *bz29* and *bz30* are both functional null alleles of calreticulin. *crt-1(bz50)* (G102E) and *crt-1(bz31)* (C133Y) encode missense mutations that affect highly conserved residues in the calreticulin signature 1 and signature 2 sequences of the N-terminal domain, respectively. Because *bz31* and *bz50* alleles confer phenotypes different from *bz29* and *bz30*, the mutant proteins they encode may have partial calreticulin function.

crt-1 Is Broadly Expressed and Functions in Affected Neurons to Influence Necrotic Cell Death

We examined the *crt-1* expression pattern using a reporter gene in which the *crt-1* promoter was fused to GFP coding sequences (Figure 3A). We found the p_{crt-1}GFP fusion protein is strongly expressed in many tissues throughout development and into adulthood, including intestine, uterus, pharynx, hypodermis, body wall muscle, and coelomocytes. Although we did observe some fluorescent neurons in animals genetically mosaic for the p_{crt-1}GFP transgene, *crt-1* did not appear strongly expressed in nervous system (data not shown). Weak signals in the nervous system might reflect the fact that the reporter construct, which lacks *crt-1* introns and 3′ untranslated regions, could be missing sequences critical for high level expression in neurons. Nonetheless, our analysis of the *crt-1* expression pattern raised the question as to whether *crt-1* acts within neurons to influence neurodegeneration or whether the gene might function indirectly, for example, by affecting muscle targets of motor neurons or hypodermal cells that surround the touch neurons.

To test whether *crt-1* function is required within the neuronal cells that undergo necrosis, we performed two experiments (Figure 3B). First, we constructed a transgene in which *crt-1* is expressed in the ventral nerve cord from the *unc-8* promoter, p_{unc-8}*crt-1*. We introduced p_{unc-8}*crt-1* into the *crt-1(bz29)*; Is[p_{unc-8}*mec-4(d)*] background and tested whether expression of *crt-1* exclu-

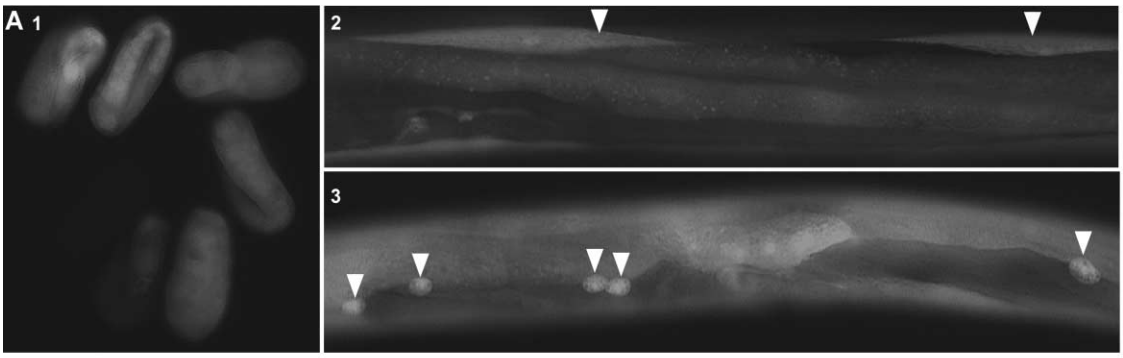

B

Introduced plasmid	Background	Degeneration
-	*crt-1(bz29)*; Is[p_{unc-8}*mec-4(d)*]	-
p_{unc-8}*crt-1*	*crt-1(bz29)*; Is[p_{unc-8}*mec-4(d)*]	+
p_{unc-8}*crt-1*	*crt-1(bz29)*; *mec-4(d)*	-
p_{unc-8}*crt-1*	wild type	-
-	*crt-1(bz29)*; *mec-4(d)*	-
p_{mec-4}*crt-1*	*crt-1(bz29)*; *mec-4(d)*	+
p_{mec-4}*crt-1*	*crt-1(bz29)*; Is[p_{unc-8}*mec-4(d)*]	-
p_{mec-4}*crt-1*	wild type	-

Figure 3. *crt-1* Is Expressed Broadly but Is Needed in Neurons for *mec-4(d)*-Induced Cell Death

(A) Expression pattern of a p_{crt-1}GFP fusion gene. All animals are genetically mosaic for the presence of the transgene, allowing visualization of a subset of the many cells that express *crt-1*. (1) Embryonic expression, (2) expression in body wall muscle (arrowheads), (3) strong expression in the coelomocytes (arrowheads), (4) expression in the uterus (arrowheads), (5) expression in the pharyngeal muscle.

(B) *crt-1* functions cell autonomously in neuronal cell death. Introduced transgenes and genetic backgrounds are as indicated. In the *crt-1;* p_{unc-8}*mec-4(d)* background, transgenics scored as positive for degeneration are >80% Unc, negative are <1% Unc, n > 100. In the *crt-1; mec-4(d)* background, transgenics scored as positive have at least 50% L1 larvae derived from transgenic roller parents with degenerating tail touch cells (this number is relatively low because all animals do not carry the transgene); negative is <2% with degenerating touch cells; n > 100.

sively in *unc-8*-expressing neurons could restore the paralyzed phenotype. In 2/2 transgenic lines we constructed, >90% of transgenic animals (as identified by the presence of co-transformation marker *rol-6(su1006)*) were paralyzed and exhibited cell swelling in the ventral nerve cord. In addition, the p_{unc-8}*crt-1* transgene was unable to rescue death suppression in the *crt-1; mec-4(d)* background, indicating cell specificity.

In a second line of experiments, we expressed the *crt-1* gene from the touch cell-specific *mec-4* promoter and tested the ability of the p_{mec-4}*crt-1* gene to restore necrosis in a *crt-1(bz29); mec-4(d)* mutant background. In 2/2 transgenic lines constructed, we observed extensive touch receptor swelling. Expression of p_{mec-4}*crt-1* in the wild-type background causes neither touch receptor swelling nor touch insensitivity. Expression of p_{mec-4}*crt-1* in the *crt-1(bz29)*; Is[p_{unc-8}*mec-4(d)*] background has no effect on locomotion or necrosis in the ventral cord. Since *crt-1* expression in affected neurons is sufficient to restore necrosis in *crt-1(bz29); mec-4(d)* and *crt-1(bz29)*; Is[p_{unc-8}*mec-4(d)*] backgrounds, it appears that *crt-1* normally functions within neurons to influence *mec-4(d)*-induced death.

Interference with Calnexin Expression also Affects *mec-4(d)*-Induced Cell Death

In the ER, luminal calreticulin works in conjunction with membrane bound calnexin to execute chaperone functions and mediate cellular Ca^{2+} homeostasis. Calreticulin and calnexin share sequence similarity in the high affinity/low capacity Ca^{2+} binding P domain (Figure 2B; Krause and Michalak, 1997). Given the functional and structural similarities between calnexin and calreticulin, we wanted to test whether calnexin might also influence *mec-4(d)*-induced necrosis. To address this question, we disrupted calnexin function using a strategy for endogenously delivered double-stranded RNA interference (RNAi) that is effective in the nervous system (Tavernarakis et al., 2000). We cloned a directly inverted repeat (IR) of a 825 bp calnexin (*cnx-1*) DNA fragment under the control of heat-inducible promoter $p_{hsp-16-2}$ and introduced the $p_{hsp16-2}$*cnx-1(IR)* gene into the *mec-4(d)* background (Figure 4A). Upon heat shock, the calnexin (IR) transcript is produced and folds back upon itself to generate double-stranded *cnx-1* RNA which specifically interferes with calnexin expression (note that the *crt-1* gene should not be targeted for degradation in this experiment because its nucleic acid similarity to calnexin is low).

When we heat-shocked adults from the Ex[$p_{hsp16-2}$*cnx-1(IR)*]; *mec-4(d)* transgenic line and counted numbers of degenerating neurons in their L1 larval stage progeny, we found significant suppression of *mec-4(d)*-induced cell death—only 56% of heat-shocked transgenic animals exhibited degeneration of one or more tail touch receptor neuron as compared to the 89% that degener-

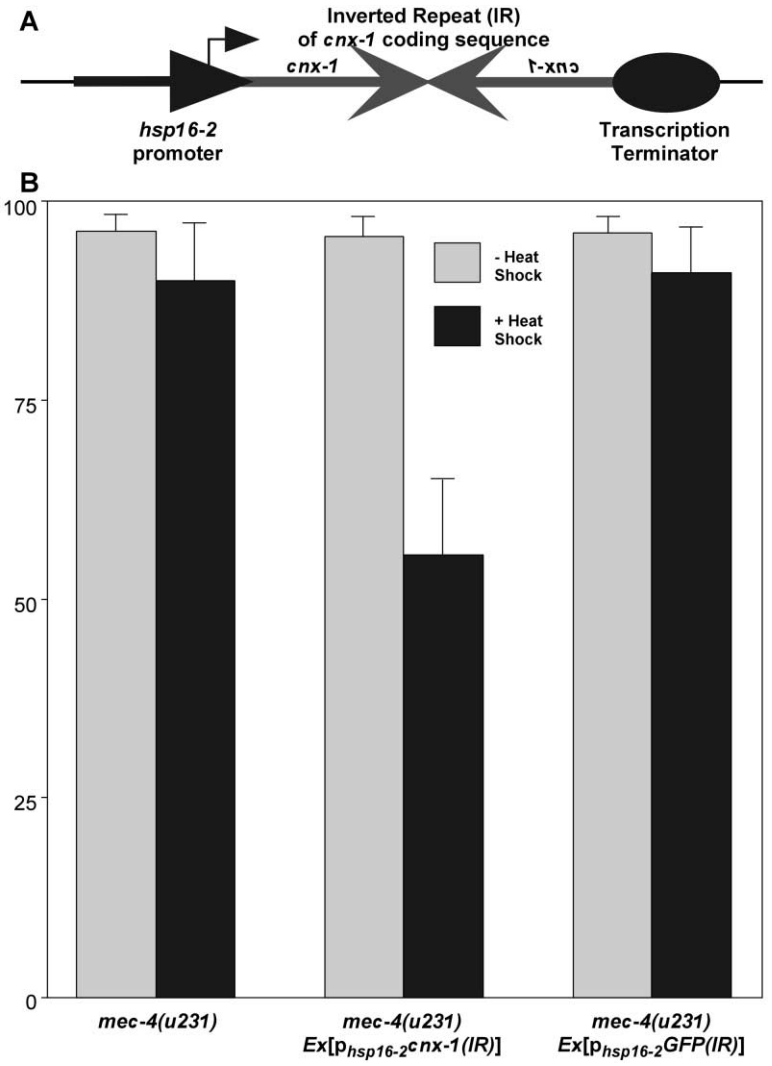

Figure 4. dsRNA Interference with Calnexin Expression Suppresses *mec-4(d)*-Induced Touch Cell Degeneration

(A) Construct designed for the in vivo inducible expression of a dsRNA hairpin. An inverted repeat (IR) containing exon-rich genomic DNA for *cnx-1* was fused to the inducible promoter *hsp16-2*. When expressed upon heat shock, the transcript is expected to form a dsRNA hairpin that induces degradation of calnexin transcripts.

(B) dsRNAi directed against calnexin has neuroprotective effects against *mec-4(d)*-induced cell death. L1 larvae of non-heat shocked or heat shocked parents of the indicated genotypes were scored for touch neuron degeneration, n > 100. The GFP(IR) gene is included as a control for the effects of expression of nonspecific dsRNA.

ated when the transgene was absent (Figure 4B). Neither the heat shock protocol itself nor the low temperature maintenance of the Ex[$p_{hsp16\text{-}2}$*cnx-1 (IR)*] exerted protective effects against necrotic-like cell death, indicating that a deficiency in calnexin itself is critical for death suppression. In addition, heat shock of a strain that carries the identical Ex[$p_{hsp16\text{-}2}$*cnx-1 (IR)*] transgene array in an otherwise wild-type background did not render offspring touch insensitive, indicating that calnexin is not required for normal MEC-4 channel function. Taken together, our results indicate that, like calreticulin, calnexin function is required for efficient *mec-4(d)*-induced neurodegeneration. Moreover, these data suggest that functions shared by calreticulin and calnexin, namely folding of glycosylated proteins and/or regulation of the ER Ca^{2+} reservoir, may be the activities critical for death suppression.

crt-1 Mutations Lower MEC-4::GFP Levels in Touch Receptor Neurons

We next sought to extend understanding of the mechanisms by which calreticulin deficiency might protect against various death stimuli by testing for effects on protein expression and effects on regulation of Ca^{2+} stores. Since calreticulin is a chaperone that facilitates the folding and translocation of many glycoproteins in the ER, and MEC-4 is glycoslylated in vitro (Lai et al., 1996), one potential mechanism for the *crt-1* suppression of *mec-4(d)*-induced cell death is that mutations in *crt-1* disrupt the biosynthesis of the toxic MEC-4(d) protein, so that fewer functional channel complexes are produced. Since in vivo assay of channel activity and quantitation of surface-expressed channel complexes are not possible in this system, we wanted to measure the amount of MEC-4 protein in various *crt-1* mutant backgrounds. It is not technically feasible to detect MEC-4 protein with antibodies in whole-mount nematode preparations or on Western blots (levels of endogenous MEC-4 channel in the touch receptors are so low that antibodies only visualize protein when it is overexpressed; low levels of channel expression are expected for mechanosensory channels which may be present in only a few copies per neuron [Lai et al., 1996]). Therefore we used GFP-tagged reporters to test possible *crt-1* effects on *mec-4* expression.

crt-1 alleles did not alter levels of a $p_{mec\text{-}4}$GFP fusion

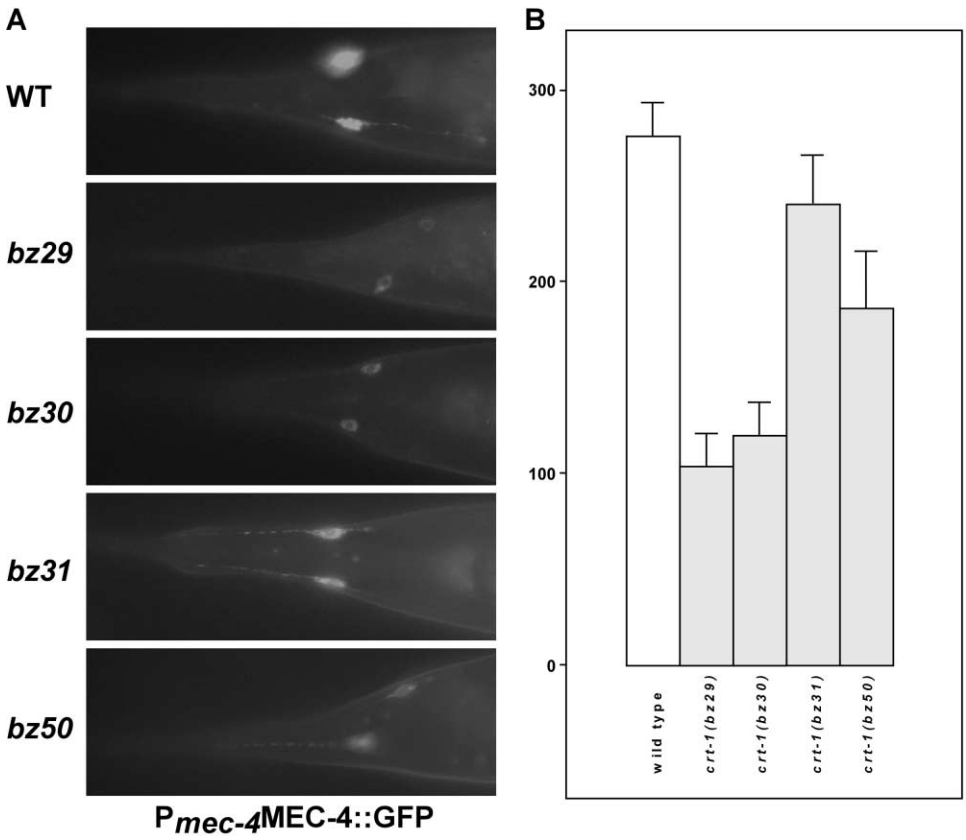

Figure 5. Mutations in *crt-1* Affect MEC-4::GFP Levels

(A) Representative photographs of MEC-4::GFP signals in *crt-1* mutant backgrounds. The same transgene array was monitored in the five genetic backgrounds indicated at left. All photographs were taken under identical exposure conditions.

(B) Quantitation of fluorescence intensity in *crt-1* mutant backgrounds. Quantitation of fluorescence of individual cells observed under identical conditions was carried out using Adobe Photoshop and the NIH Image algorithm. Numbers cited are the average of 20 tail touch neurons scored.

protein that contains only a few N-terminal MEC-4 amino acids and is expressed using all 5′ regulatory regions required for touch cell-specific synthesis (Mitani et al., 1993) and for rescue of a *mec-4* mutant when driving expression of the *mec-4* gene (Hong and Driscoll, 1994). Thus, we infer that *crt-1* mutations do not markedly affect *mec-4* transcription. *crt-1* mutations can, however, reduce the levels of a full-length MEC-4 channel subunit tagged with GFP at the C terminus, a protein that should sort and initiate channel assembly in the ER (Figure 5). The *bz29* and *bz30* putative null mutations, which exert the strongest death-suppressing effects in touch neurons, exhibited the lowest levels of MEC-4::GFP fluorescence (approximately 30% of wild-type levels). Alleles *bz31* and *bz50*, which do not suppress degeneration in touch cells, did not markedly affect MEC-4::GFP protein levels. Thus, a plausible factor in efficient *crt-1*(null) suppression of endogenous *mec-4(d)* toxicity is lowered production of a toxic channel.

We note, however, that *crt-1* null alleles do not render animals touch insensitive (Table 1C) and thus, even in the absence of calreticulin, the MEC-4 touch channel must be assembled and expressed to a degree sufficient for mechanosensory function. Also, even when the *mec-4(d)* gene dosage is decreased to 1/3 of the wild-type dosage (Herman, 1987), extensive degeneration still occurs. These observations, in conjunction with the fact that cell death in strain BZ7, which has 10× *mec-4(d)* gene dosage and exhibits accelerated degeneration (presumably due to elevated expression of the toxic channel in touch neurons), is efficiently suppressed by strong *crt-1* alleles (Table 1B), hint that an apparent reduction to approximately 1/3 normal MEC-4 protein levels might not be sufficient to explain the essentially complete block of *mec-4(d)*-induced cell death that is observed in the *crt-1* null backgrounds. Given these concerns, we sought to address whether the role of calreticulin in cellular Ca^{2+} homeostasis might also contribute to neurodegeneration.

Disruption of Cellular Ca^{2+} Balance Can Suppress *mec-4(d)* Toxicity without Changing MEC-4::GFP Levels

Ca^{2+} binding calreticulin plays a critical and complex role in cellular calcium homeostasis as a major site for stored Ca^{2+} (Michalak et al., 1999), and Ca^{2+} is known to contribute in pivotal ways in mammalian cell death (Choi, 1992; Leist and Nicotera, 1998). Thus, we also sought to address whether the role of calreticulin in Ca^{2+} regulation might also contribute to neurodegeneration.

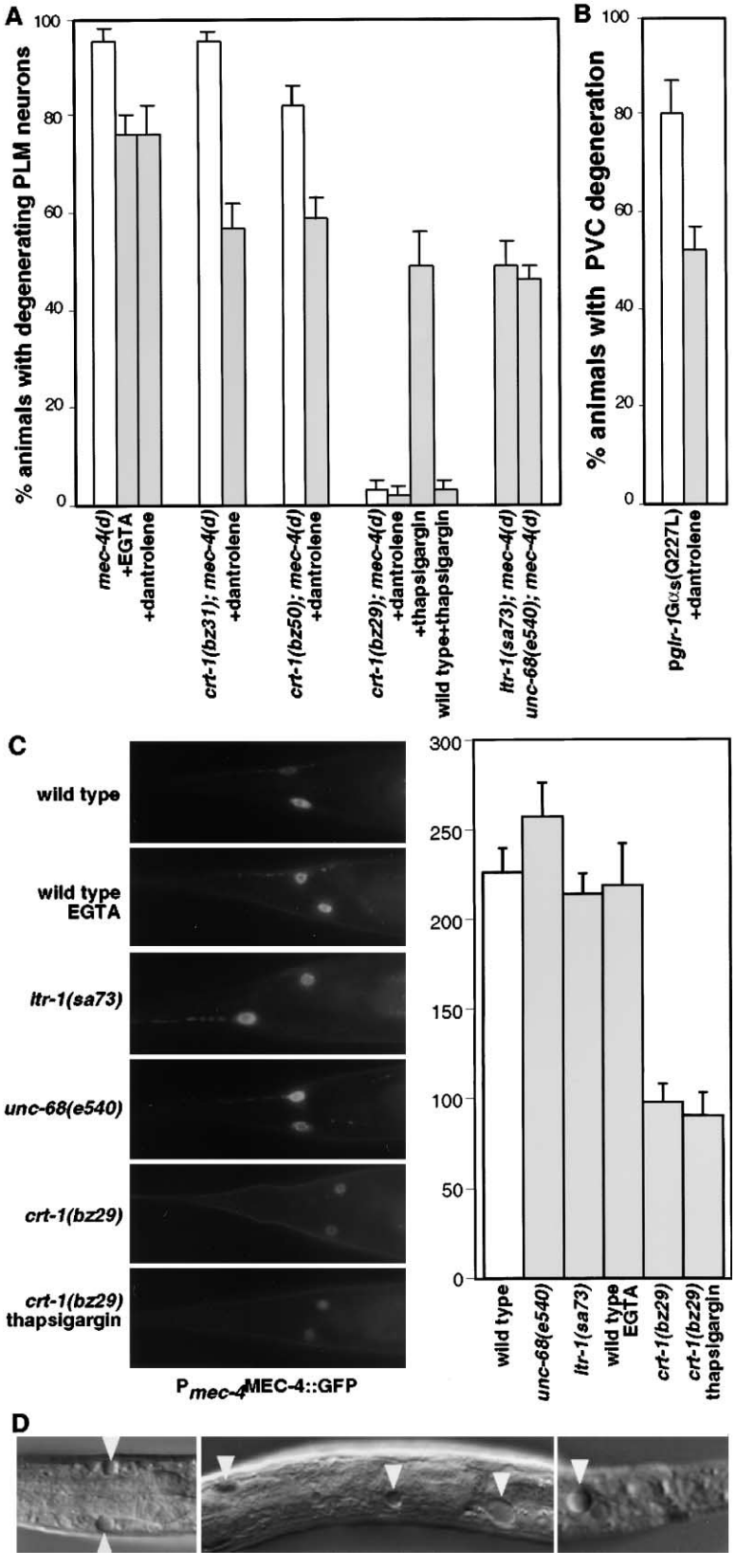

Figure 6. Manipulation of ER Ca^{2+} Release Affects *mec-4(d)*-Induced Degeneration and Can Bypass the *crt-1*-Induced Block of Cell Death

(A) Pharmacological and genetic manipulation of $[Ca^{2+}]$ influence cell death. Protocols designed to reduce cellular $[Ca^{2+}]$ (EGTA, 50 mM), prevent release of ER stores (dantrolene, 10 μM), provoke release of ER stores and inhibit ER reuptake (thapsigargin, 3 μg/ml), or genetically diminish release of ER Ca^{2+} (mutant IP3 receptor *itr-1(sa73)* and mutant ryanodine receptor *unc-68(e540)*) were assayed for their abilities to influence PLM tail touch receptor cell death in the genetic backgrounds indicated. $n > 100$ animals scored for each assay; assay of *itr-1; mec-4(d)* performed at 25°C.

(B) Dantrolene (10 μM) also protects against $p_{glr\text{-}1}G\alpha_s$(Q227L)-induced PVC degeneration. $n > 100$ animals were scored for PVC degeneration as described in Table 1(i).

(C) Quantitation of MEC-4::GFP fluorescence intensity in strains with altered Ca^{2+} homeostasis. Left, representative photographs of MEC-4::GFP signals in various mutant backgrounds. The same transgene array was monitored in animals treated as in (A). All photographs were taken under identical exposure conditions. Right, quantitation of fluorescence of individual cells observed under identical conditions was carried out using Adobe Photoshop and the NIH Image algorithm. Numbers cited are the average of 20 tail touch neurons scored.

(D) Thapsigargin-driven release of ER Ca^{2+} stores can induce necrosis. Arrows indicate necrotic figures in a wild-type animal hatched in the presence of 3 μg/ml thapsigargin.

Calreticulin is a major storage site for Ca^{2+} in the ER in nonmuscle cells. Ca^{2+} is released from ER stores into the cytoplasm via the inositol triphosphate receptor (InsP3R) and the ryanodine receptor (RyR) Ca^{2+} channels and is returned to the ER from the cytoplasm by the SERCA Ca^{2+} pump (Pozzan et al., 1994). We tested

for potential influences of Ca^{2+} in *mec-4(d)*-induced degeneration in two ways: we used chemical reagents to manipulate ER Ca^{2+} release and we tested genetic mutations that alter release of ER Ca^{2+} stores (Figure 6A).

We first treated *mec-4(d)* mutants with EGTA, a Ca^{2+}-specific chelator. In L1 larvae of treated parents, *mec-4(d)*-induced touch receptor degeneration was reduced to 76% (wild-type animals are mobile and touch sensitive under these conditions), an initial indication that perturbing cellular [Ca^{2+}] could be protective against the *mec-4(d)*-induced insult. We next tested whether Ca^{2+} derived from ER stores might be important for necrosis. We treated *mec-4(d)* mutants with dantrolene, a reagent that specifically inhibits Ca^{2+} release from ER stores (Song et al., 1993). In progeny of dantrolene-treated animals, degeneration was reduced to 76%, consistent with the hypothesis that contributions of ER Ca^{2+} stores are important for the progression of necrosis. Dantrolene treatment also enhanced degeneration suppression in the weak *crt-1(bz31)* and *crt-1(bz50)* point mutants.

In a complementary genetic approach, we tested the effects of mutations in the InsP3R and the RyR ER Ca^{2+} release channel genes on *mec-4(d)*-induced degeneration. We crossed a partial loss-of-function mutation in InsP3R, *itr-1(sa73)* (Dal Santo et al., 1999), into the *mec-4(d)* background and found that the double mutant exhibited a significant suppression of degeneration (49% touch cells degenerate). In addition, we found that a double mutant of RyR *unc-68(e540)* (Maryon et al., 1996) and *mec-4(d)* was significantly suppressed for cell death (46% touch cells degenerate).

Since pharmacological and genetic manipulation of Ca^{2+} could influence the production of the MEC-4 protein, we quantitated MEC-4::GFP fluorescence under the conditions of altered Ca^{2+} homeostasis tested (Figure 6C). We found that neither treatment with EGTA nor genetic mutations in *itr-1* or *unc-68,* which are conditions that significantly suppress *mec-4(d)*-induced death, detectably affected the levels of MEC-4::GFP. Moreover, touch sensitivity is normal in *itr-1* and *unc-68* backgrounds (data not shown). Thus, a reduced amount of MEC-4 is unlikely to explain death suppression effects in these experiments. Rather, our data suggest that normal release of ER Ca^{2+} stores is needed for efficient *mec-4(d)*-induced neurodegeneration and they indicate that both InsP3R and RyR Ca^{2+} release channels can contribute to this process. Further support of a general role of ER Ca^{2+} release in necrotic cell death is that dantrolene treatment can significantly reduce the extent of PVC degeneration in the *nuIs5*[$p_{glr\text{-}1}G\alpha_s$ *(Q227L)* strain (Figure 6B).

If high $[Ca^{2+}]_i$ or Ca^{2+} release itself is a critical aspect of *mec-4(d)*-induced degeneration that is disrupted when calreticulin is absent, then experimentally driven ER Ca^{2+} release might overcome the *crt-1*-induced block on cell death. We sought to reverse *crt-1* death suppression by driving release of remaining ER Ca^{2+} stores in the *crt-1(bz29); mec-4(d)* double mutant background (Figure 6A). We treated *crt-1(bz29); mec-4(d)* double mutants, which are fully suppressed for necrotic-like cell death, with thapsigargin, which both inhibits the SERCA ER Ca^{2+} re-uptake pump and induces release of ER Ca^{2+} via an InsP3 receptor-independent mechanism (Takemura et al., 1989). Thapsigargin treatment restored a significant level of touch cell necrosis in the offspring of *crt-1(bz29); mec-4(d)* mutants (49% of treated animals have degenerating touch neurons). Importantly, this restoration of death is not accompanied by apparent changes in MEC-4::GFP levels (Figures 6A and 6C), again underscoring that changes in Ca^{2+} levels, rather than changes in MEC-4 levels, are critical for death suppression. Interestingly, we found that thapsigargin treatment of wild-type animals induces vacuoles that resemble necrotic-like cell deaths in random cells (Figure 6D). Counts of numbers of fluorescent neuronal cell bodies in progeny of untreated $p_{unc\text{-}129}$GFP animals (0 of 11 neurons scored are missing in >1000 animals scored) to thapsigargin-treated animals (4 neuronal cell bodies missing in 120 animals scored) suggest that some cells actually die as a consequence of thapsigargin treatment. These data suggest that elevation of $[Ca^{2+}]_i$ itself could be cytotoxic in nematodes and support a model in which a critical rise in $[Ca^{2+}]_i$ is a causative factor in neurotoxicity.

Discussion

In a *C. elegans* mutant lacking calreticulin, necrotic-like cell death induced by the MEC-4(d) and DEG-1(d) hyperactivated ion channels or by constitutively activated $G\alpha_s$ is suppressed. We suggest that both defects in calreticulin chaperone function and in maintenance of Ca^{2+} homeostasis contribute to the efficient block of *mec-4(d)*-induced cell death of the touch receptor neurons. Since a likely null *crt-1* mutation can reduce levels of a tagged MEC-4::GFP protein, we infer that reduced expression of the toxic channel itself (or of a key death protein) may contribute to full neuroprotection of touch receptor neurons. The critical contribution of disrupted Ca^{2+} homeostasis is suggested by our findings that deficiencies in ER Ca^{2+} binding proteins calreticulin and calnexin, as well as mutations altering the InsP3R and RyR ER Ca^{2+}-release channels, all significantly suppress *mec-4(d)*-induced cell death (the latter two suppress without detectably altering MEC-4::GFP levels). Together with data on pharmacological manipulation of intracellular Ca^{2+} levels, our data strongly implicate high $[Ca^{2+}]_i$ in necrotic cell death.

A Viable Calreticulin Mutant in *C. elegans*

Calreticulin is known to influence a variety of fundamentally important biological processes (Michalak et al., 1999; Llewellyn et al., 2000). We have shown that *crt-1* is expressed in most, if not all, *C. elegans* cells from early in development until late into the lifespan. A likely nematode null mutant of calreticulin, however, is viable, fertile at 20°C, and exhibits only modest defects in development or in the behaviors we assayed. The *crt-1* deficiency does confer pleiotrophic abnormalities that include slowed growth and reduced body size (sperm defects that may cause sterility have also been noted at 25°C (Park et al., 2001)). In mouse, calreticulin is needed for heart and brain development and is thus essential for viability (Mesaeli et al., 1999; Rauch et al., 2000), although both embryonic stem cells and fibroblasts from $crt^{-/-}$ mutants can be cultured (Coppolino

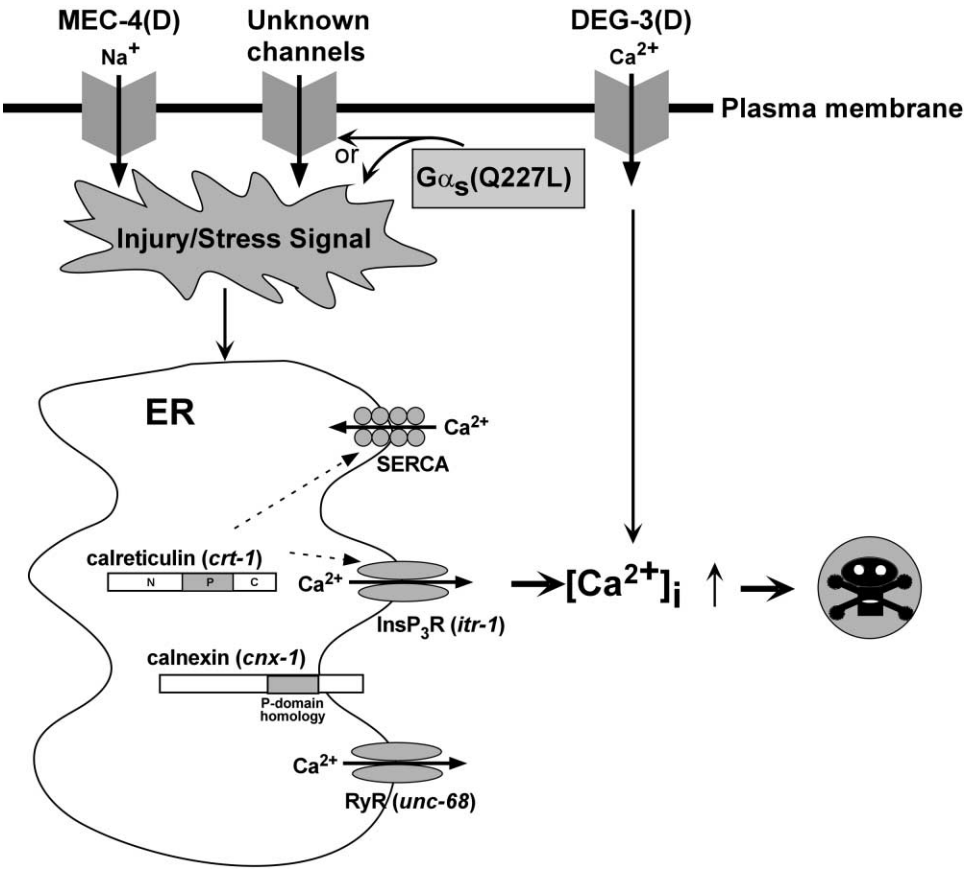

Figure 7. Working Model for Channel-Mediated Neurotoxicity in *C. elegans*

In the case of the hyperactivated MEC-4(d) degenerin channel, elevated Na^+ influx signals directly, or generates a signal that provokes, release of Ca^{2+} from ER stores. The resultant $[Ca^{2+}]_i$ increase is essential for downstream events that cause cellular demise. Mutations affecting ER calcium storage (calreticulin and calnexin) or ER calcium release (IP3 and RYR receptor Ca^{2+} release channels) disrupt release and are therefore neuroprotective. Constitutively activated $G\alpha_s$(G227L) may signal via ACY-1 adenyl cyclase to hyperactivate ion channels and provoke ER Ca^{2+} release via a mechanism in common with MEC-4(d). The plasma membrane DEG-3(d) channel directly conducts increased Ca^{2+} and thus raises $[Ca^{2+}]_i$ to toxic levels without an essential Ca^{2+} release from the ER.

et al., 1997; Mesaeli et al., 1999). As the first viable calreticulin mutants, the *C. elegans crt-1* strains we describe constitute critical reagents for in vivo genetic, molecular, and biochemical analysis of the complexities of calreticulin function.

Calreticulin Structure/Function

Calreticulin has three distinct structural and functional domains: (1) a highly conserved N domain, which binds Zn^{2+} (Baksh et al., 1995) and mediates interactions with several proteins, including ER proteins with chaperone activity (see Michalak et al., 1999); (2) a calnexin-homologous proline-rich P domain that functions as a high-affinity Ca^{2+} binding domain (Baksh and Michalak, 1991) and has lectin-like chaperone activity (Vassilakos et al., 1998); and (3) an acidic C domain that acts as a high-capacity Ca^{2+} binding domain (Baksh and Michalak, 1991). Our death-suppressor screen identified the first known missense mutations in calreticulin, which encode distinct single amino acid substitutions for highly conserved residues in the N domain (*bz31,* C133Y; *bz50,* G102E). The C133Y substitution directly affects a highly conserved Cys residue that participates in intramolecular disulfide bond within the N domain (Matsuoka et al., 1994), and thus *crt-1(bz31)* is expected to encode a protein lacking this structure. The potential impact of the G102E substitution is impossible to predict due to a paucity of structure/function information on calreticulin. Because *bz31* and *bz50* have distinct genetic properties from the likely null alleles, it appears the proteins they encode (which can be immunologically detected; J. Ahnn, personal communication) retain partial function. We speculate that the G102E and C133Y proteins may specifically disrupt the function(s) of the conserved N-terminal domain but retain Ca^{2+} binding and other properties of the P and C domains, which could account for their lessened capacities to suppress against strong neurotoxic stimuli.

Modeling Channel-Mediated Neurotoxicity in *C. elegans*

Our data suggest that $[Ca^{2+}]_i$, as regulated by calreticulin's Ca^{2+} storage and release capacities, plays an essential role in a necrotic-like cell death caused by hyperactive Na^+ channels in *C. elegans*. Genetic evidence also indicates that Ca^{2+} release from ER by both InsP3R

(*itr-1*) and RyR (*unc-68*) channels play important functions in this neurotoxicity, and chemically driven Ca^{2+} release can overcome the *crt-1* block of cell death, suggesting that release of Ca^{2+} itself may be a critical step in the death mechanism. Taken together, our data suggest a working model for necrotic cell death initiated by hyperactivation of degenerin Na^+ channels in *C. elegans* (Figure 7). Mutant degenerin channels cause excess Na^+ to enter neurons. This injury signal may act directly to elicit an influx of Ca^{2+} from ER stores (much of which is stored bound to calreticulin). Elevated $[Ca^{2+}]_i$ may then activate cellular enzymes/proteins that dismantle the cell. Alternatively, steady state Ca^{2+} levels, maintained by Ca^{2+} storage and release proteins, may be critical to one or more steps involved in neurotoxicity. The experimental distinction between dynamic versus steady state models of Ca^{2+} changes must await refinement of accurate methods for measurement of Ca^{2+} fluxes in tiny *C. elegans* neurons (Kerr et al., 2000). In support of a dynamic model, however, is a report that in calreticulin-deficient mouse cells, overall cytoplasmic $[Ca^{2+}]_i$ is not affected but InsP3R-dependent release of Ca^{2+} stores is markedly diminished (Mesaeli et al., 1999).

This model can also accommodate our observations of *crt-1* influence on other necrosis-inducing stimuli. In the case of $G\alpha_s$(Q227L), the mutant G protein may signal directly to provoke ER Ca^{2+} release or may hyperactivate ion channels which, like MEC-4(d), elicits ER Ca^{2+} release; downstream events required for cell death would be common with MEC-4(d). In the case of the DEG-3(d) channel that does not require calreticulin for toxicity, excess Ca^{2+}, rather than Na^+, is transported directly into the cell—thus the mutant channel may directly elevate Ca^{2+} in the appropriate cellular compartment to trigger cell death. Analysis of additional proteins required for necrotic cell death that are encoded by other suppressor genes identified in our screen and measurement of temporal changes in $[Ca^{2+}]_i$ during necrosis should help fill in details of the death mechanism.

Necrotic Cell Death Mechanisms May Be Conserved from *C. elegans* to Humans

In mammalian excitotoxic cell death, excess glutamate released into the synaptic cleft hyperactivates glutamate-gated channels on postsynaptic neurons (see Choi, 1992). Of these glutamate-gated channels, kainate and AMPA receptor channel subtypes conduct Na^+ and NMDA receptor channels, which play a key role in excitotoxicity, conduct both Na^+ and Ca^{2+}. Plasma membrane depolarization caused by the Na^+ influx may activate voltage-gated Ca^{2+} channels in the plasma membrane to increase $[Ca^{2+}]_i$. However, although Ca^{2+} influx is required for excitotoxic cell death, questions have arisen as to whether the rise in $[Ca^{2+}]_i$ can be accounted for solely by influx from extracellular Ca^{2+} sources alone. Indeed, some evidence supports that the initial Ca^{2+} entry may provoke Ca^{2+}-dependent Ca^{2+} release from the ER and that ER Ca^{2+} stores contribute critically to toxic Ca^{2+} levels in injured neurons (reviewed in Mody and MacDonald, 1995; Mattson et al., 2000). For example, in mammalian neurons, dantrolene (which blocks ER Ca^{2+} release) can block most of the Ca^{2+} rise produced by NMDA receptor activation and can protect against excitotoxicity in vitro (Frandsen and Schousboe, 1991, 1993; Lei et al., 1992; Segal and Manor, 1992). Dantrolene has also been noted to have neuroprotective effects on in vivo models of excitotoxicity (Nagatomo et al., 2001), ischemia (Zhang et al., 1993), and traumatic brain injury (Weber et al., 1999).

Our work thus extends the known similarities between *mec-4(d)*-induced cell death in *C. elegans* and mammalian excitotoxic cell death, which share (1) initiation of toxicity by hyperactivated channels that conduct Na^+, (2) a requirement for Ca^{2+} release from the ER, and (3) a necrotic morphological type. Overall, the remarkable parallels between ion channel-induced toxicity in nematodes and humans suggest that critical aspects of necrotic cell death may be conserved from nematodes to humans. If so, this work both underscores the potential of the *C. elegans* system to identify key targets for therapeutic intervention and suggests that a focused effort to regulate ER Ca^{2+} release consequent to neuronal injury could be of clinical importance.

Experimental Procedures

C. elegans Strains

Methods for maintaining/crossing/mutagenizing *C. elegans* strains were as described by Brenner (1974). Unless indicated, strains were cultured at 20°C. The following genetic markers and mutant strains were used in this study: LGII, *unc-105(n1274)*; LGIV, *unc-8(n491)*, *itr-1(sa73)*; LGV, *dpy-11(e224)*, *crt-1(bz29, bz30, bz31, bz50)*, *unc-68(e540)*, *deg-3(u662)*, BC277[*unc-46(e177) dpy-11(e224)*], BW1943 [*gad-1(ct226) dpy-11(e224)*], BC364[*dpy-11(e224) unc-68(e540)*]; LGX, *deg-1(u38), mec-4(u231)*. *nDf18* and *adDf1059* are two deficiencies on LGV that delete markers flanking *crt-1*. RW7000 is the Bergerac strain used in Tc1 polymorphism mapping. Integrated transgenic strains were ZB194 *bz32*Is[p_{unc-8}*mec-4(d)*]I (this study), KP742 *nuIs5*[p_{glr-1} $G\alpha_s$(Q227L) p_{glr-1}GFP] (Berger et al., 1998), ZB7 *bzIs3*[p*mec-4(d)*]X (Hall et al., 1997), NW1099 *Is*[$p_{unc-129/SmaI}$GFP] (Colavita et al., 1998). Transgenic strains were constructed by injecting plasmids at 50 ng/μl and cosmids at 10 ng/μl unless otherwise indicated (Mello and Fire, 1995). The p_{unc-8}*mec-4(d)* transgenic array was integrated using UV irradiation at 500 J/m^2. Note that injection of a full-length p_{crt-1}CRT-1::GFP plasmid at 50 ng/μl appeared to be lethal: fluorescent eggs could be easily identified, but none of them hatched; $n > 200$.

Genetic Characterization of *crt-1*

Alleles *bz29*, *bz30*, *bz31*, and *bz50* were initially mapped to chromosome V close to *stP192* (map position 0.00) by STS polymorphism mapping (Williams et al., 1992)—the *stP192* polymorphism was detected in 1/29 *bz29* homozygotes. Using three-factor mapping, *bz31* was mapped between *unc-46* and *dpy-11*, probably to the left of *gad-1*: 1/9 Dpy Non-Unc recombinants segregated *bz31*; 3/3 Dpy Non-Gad recombinants segregated *bz31*. Deficiency analysis narrowed the candidate region into an interval between *nDf18* and *adDf1059*.

Phenotypic Characterization of Suppressor Mutants

All *de*generation suppressor (*des*) mutations counter the deleterious effects of the dominantly acting Is[p_{unc-8}*mec-4(d)*] array rather than delete the toxic transgene since transgene-specific sequences can be amplified from all suppressed lines and crossing wild-type males to the *des*; Is[p_{unc-8}*mec-4(d)*] mutants caused the Unc phenotype to reappear in *des*/+; Is[p_{unc-8}*mec-4(d)*]/+ cross progeny heterozygotes. Neurodegeneration of tail touch neurons was scored as in Chung et al., 2000. The *deg-1(d), deg-3(d)*, and $G\alpha_s$-induced vacuolated cell phenotypes were scored using Nomarski DIC microscopy (Driscoll, 1995). Toxicity of $G\alpha_s$(Q227L) was evaluated by scoring the number of *nuIs5* animals that had viable GFP-labeled PVC interneurons; thapsigargin effects on viable cells were performed by checking for fluorescent DA and DB motorneurons (except DA8

and DA9) in progeny of treated parents. Touch sensitivity of *crt-1* mutants was assayed by stimulating young adults with an eyebrow hair in two consecutive alternating touches to the anterior and posterior (Chalfie and Sulston, 1981). Animals responding to all stimuli at both positions were scored as positive. For sustained touch sensitivity, animals were touched at mid-body for five consecutive times. Those that responded at least three times out of five were scored as positive. Body size was measured using the NIH image algorithm. Brood size was determined by counting the total number of offspring from single hermaphrodites. Generation time was determined by allowing adult hermaphrodites to lay eggs for 1 hr, then removing them from the plates. The plates were monitored to determine when the first F1 generation parents initiated egglaying. The defecation period was assayed in L4 animals as the time interval between one posterior body contraction to the next (Thomas, 1990). For each strain, ten different animals were assayed for ten cycles. All behavioral assays were performed three independent times.

Molecular Constructs

Sequencing analysis was performed by DNA Core Facility at UMDNJ (Piscataway, NJ). *crt-1* coding sequences were verified using available EST data. To construct the $p_{crt\text{-}1}$GFP reporter gene, a 1479 bp fragment of *crt-1* promoter sequences (corresponding to sequences between 45353 and 46814 in the Y38A10A cosmid, accession number AF125963) was amplified from N2 genomic DNA using primers 5′-GCAGCCCGGGTTCATTTCGTTTTTCGATA-3′ and 5′-AGATCTG CAGGTGAACCGAGCCCGAGTAG-3′, digested with PstI and SmaI, then ligated into GFP vector pPD95.77 (see the ciw vector archive at www. ciwemb.edu). For the construction of $p_{mec\text{-}4}$MEC-4::GFP fusion gene, a 4.7 kb HindIII-BamHI fragment including the *mec-4* promoter and coding sequences for amino acids 1–760 (derived from TU#44, Mitani et al., 1993) was inserted into pPD95.77. For the construction of $p_{unc\text{-}8}$*crt-1*, a 1.4 kb fragment from the *unc-8* promoter was amplified from $p_{unc\text{-}8}$*mec-4(d)* (Harbinder, et al., 1997) using primers 5′-GATGGATCCGGGAGCATTTCCGGTAGTT-3′ and 5′-ACCCT GCAGCCATTGATTCTGGTTCATGG-3′, digested and ligated into pBluescript II KS(-) vector using BamHI and PstI sites, generating pKSu. Similarly, for $p_{mec\text{-}4}$*crt*-1, a 1.0 kb fragment of *mec-4* promoter was amplified from TU#44 using primers 5′-ATTTCTAGACCGTCT GAACATAAAATTAGT-3′ and 5′-AAACTGCAGACATGTACTCGGAT GGGTC-3′, digested and ligated into pBluescript II KS(-) vector using XbaI and PstI sites, generating pKSm. A 1.8 kb fragment containing the *crt-1* coding sequences and 3′UTR (corresponding to sequences between 43562 and 45359 in the Y38A10A cosmid) was amplified from N2 genomic DNA using primers 5′-AACTGCA GAAATGAAATCACTCTGCCTGTTAGCAA-3′ and 5′-GGGGTACCC GGACGAGTTGGTCGCGATGGATG-3′, digested with PstI and KpnI, then inserted into pKSu and pKSm, generating $p_{unc\text{-}8}$*crt-1* and $p_{mec\text{-}4}$*crt-1*, respectively. RNAi foldback plasmid $p_{hsp16\text{-}2}$*cnx-1*IR was constructed by amplifying two 825 bp fragments both containing the last 2 exons of *cnx-1* (corresponding to sequences between 17749 and 18556 in the ZK632 cosmid, accession number Z22181) from N2 genomic DNA using primer pairs 5′-TTGGAGCTCATCTCG TGATCAATCCCCTC-3′ and 5′-CTTGGATCCCAGGGAAAATGGAT TCGACC-3′, 5′-TTGGGTACCATCTCGTGATCAATCCCCTC-3′ and 5′-CTTGGATCCCAGGGAAAATGGATTCGACC-3′, respectively, digesting with SacI, BamHI and KpnI, BamHI, respectively, and ligating into KpnI, SacI-digested pPD49.78 vector (Mello and Fire, 1995).

RNAi Procedures

For dsRNA interference with the *cnx-1* gene in *mec-4(u231)*, 100 transgenic roller young adults from lines harboring $p_{hsp16\text{-}2}$*cnx-1*IR (or $p_{hsp16\text{-}2}$GFPIR control) plus pRF4 were reared continuously at 20°C (non-heat shock), or heat shocked for 4 hr at 35°C, before returning to 20°C. Progeny of heat shocked animals and non-heat shocked controls were scored for degenerating touch cells at the L1 stage.

Acknowledgments

We thank G. Patterson and A. Singson for critical reading of the manuscript. We are indebted to J. Ahnn for communication of results prior to communication and strain comparisons and to J. Kaplan and A. Hart for strains. Some nematode strains used in this work were provided by the Caenorhabditis Genetics Center, which is funded by the NIH National Center for Research Resources (NCRR). This work was funded by grants from the NIH (NS34435) and the Amyotrophic Lateral Sclerosis Society of America.

Received February 12, 2001; revised June 29, 2001.

References

Adams, C.M., Snyder, P.M., Price, M.P., and Welsh, M.J. (1998). Protons activate brain Na^+ channel 1 by inducing a conformational change that exposes a residue associated with neurodegeneration. J. Biol. Chem. *273*, 30204–30207.

Baksh, S., and Michalak, M. (1991). Expression of calreticulin in *Escherichia coli* and identification of its Ca^{2+} binding domains. J. Biol. Chem. *266*, 21458–21465.

Baksh, S., Spamer, C., Heilmann, C., and Michalak, M. (1995). Identification of the Zn^{2+} binding region in calreticulin. FEBS Lett. *376*, 53–57.

Berger, A.J., Hart, A.C., and Kaplan, J.M. (1998). G-alphas-induced neurodegeneration in *Caenorhabditis elegans*. J. Neurosci. *18*, 2871–2880.

Brenner, S. (1974). The genetics of *Caenorhabditis elegans*. Genetics *77*, 71–94.

Chalfie, M., and Sulston, J. (1981). Developmental genetics of the mechanosensory neurons of *Caenorhabditis elegans*. Dev. Biol. *82*, 358–370.

Chalfie, M., and Wolinsky, E. (1990). The identification and suppression of inherited neurodegeneration in *Caenorhabditis elegans*. Nature *345*, 410–416.

Choi, D.W. (1992). Excitotoxic cell death. J. Neurobiol. *23*, 1261–1276.

Chung, S., Gumienny, T.L., Hengartner, M.O., and Driscoll, M. (2000). A common set of engulfment genes mediates removal of both apoptotic and necrotic cell corpses in *C. elegans*. Nat. Cell Biol. *2*, 931–937.

Clarke, P.G. (1990). Developmental cell death: morphological diversity and multiple mechanisms. Anat. Embryol. *181*, 195–213.

Colavita, A., Krishna, S., Zheng, H., Padgett, R.W., and Culotti, J.G. (1998). Pioneer axon guidance by UNC-129, a *C. elegans* TGF-beta. Science *281*, 706–709.

Coppolino, M.G., Woodside, M.J., Demaurex, N., Grinstein, S., St-Arnaud, R., and Dedhar, S. (1997). Calreticulin is essential for integrin-mediated calcium signalling and cell adhesion. Nature *386*, 843–847.

Dal Santo, P., Logan, M.A., Chisholm, A.D., and Jorgensen, E.M. (1999). The inositol trisphosphate receptor regulates a 50-second behavioral rhythm in *C. elegans*. Cell *98*, 757–767.

Driscoll, M. (1995). Methods for the study of cell death in the nematode *Caenorhabditis elegans*. Methods Cell Biol. *46*, 323–353.

Driscoll, M., and Chalfie, M. (1991). The *mec-4* gene is a member of a family of *Caenorhabditis elegans* genes that can mutate to induce neuronal degeneration. Nature *349*, 588–593.

Frandsen, A., and Schousboe, A. (1991). Dantrolene prevents glutamate cytotoxicity and Ca^{2+} release from intracellular stores in cultured cerebral cortical neurons. J. Neurochem. *56*, 1075–1078.

Frandsen, A., and Schousboe, A. (1993). Excitatory amino acid-mediated cytotoxicity and calcium homeostasis in cultured neurons. J. Neurochem. *60*, 1202–1211.

Garcia-Anoveros, J., Ma, C., and Chalfie, M. (1995). Regulation of *Caenorhabditis elegans* degenerin proteins by a putative extracellular domain. Curr. Biol. *5*, 441–448.

Garcia-Anoveros, J., Garcia, J.A., Liu, J.D., and Corey, D.P. (1998). The nematode degenerin UNC-105 forms ion channels that are activated by degeneration- or hypercontraction-causing mutations. Neuron *20*, 1231–1241.

Hall, D.H., Gu, G., Garcia-Anoveros, J., Gong, L., Chalfie, M., and Driscoll, M. (1997). Neuropathology of degenerative cell death in *Caenorhabditis elegans*. J. Neurosci. *17*, 1033–1045.

Harbinder, S., Tavernarakis, N., Herndon, L.A., Kinnell, M., Xu, S.Q., Fire, A., and Driscoll, M. (1997). Genetically targeted cell disruption in *Caenorhabditis elegans*. Proc. Natl. Acad. Sci. USA *94*, 13128–13133.

Hardy, J., and Gwinn-Hardy, K. (1998). Genetic classification of primary neurodegenerative disease. Science *282*, 1075–1079.

Hong, K., and Driscoll, M. (1994). A transmembrane domain of the putative channel subunit MEC-4 influences mechanotransduction and neurodegeneration in *C. elegans*. Nature *367*, 470–473.

Herman, R.K. (1987). Mosaic analysis of two genes that affect nervous system structure in *C. elegans*. Genetics *116*, 377–388.

Kerr, J.F., Wyllie, A.H., and Currie, A.R. (1972). Apoptosis: a basic biological phenomenon with wide-ranging implications in tissue kinetics. Br. J. Cancer *26*, 239–257.

Kerr, R., Lev-Ram, V., Baird, G., Vincent, P., Tsien, R.Y., and Schafer, W.R. (2000). Optical imaging of calcium transients in neurons and pharyngeal muscle of *C. elegans*. Neuron *26*, 583–594.

Korswagen, H.C., Park, J.H., Ohshima, Y., and Plasterk, R.H. (1997). An activating mutation in a *Caenorhabditis elegans* Gs protein induces neural degeneration. Genes Dev. *11*, 1493–1503.

Krause, K.H., and Michalak, M. (1997). Calreticulin. Cell *88*, 439–443.

Lai, C.C., Hong, K., Kinnell, M., Chalfie, M., and Driscoll, M. (1996). Sequence and transmembrane topology of MEC-4, an ion channel subunit required for mechanotransduction in *Caenorhabditis elegans*. J. Cell Biol. *133*, 1071–1081.

Lee, J.M., Zipfel, G.J., and Choi, D.W. (1999). The changing landscape of ischaemic brain injury mechanisms. Nature *399*, A7–A14.

Lei, S.Z., Zhang, D., Abele, A.E., and Lipton, S.A. (1992). Blockade of NMDA receptor-mediated mobilization of intracellular Ca^{2+} prevents neurotoxicity. Brain Res. *598*, 196–202.

Leist, M., and Nicotera, P. (1998). Calcium and neuronal death. Rev. Physiol. Biochem. Pharmacol. *132*, 79–125.

Liu, J., Schrank, B., and Waterston, R.H. (1996). Interaction between a putative mechanosensory membrane channel and a collagen. Science *273*, 361–364.

Llewellyn, D.H., Johnson, S., and Eggleton, P. (2000). Calreticulin comes of age. Trends Cell Biol. *10*, 399–402.

Martin, L.J., Al-Abdulla, N.A., Brambrink, A.M., Kirsch, J.R., Sieber, F.E., and Portera-Cailliau, C. (1998). Neurodegeneration in excitotoxicity, global cerebral ischemia, and target deprivation: A perspective on the contributions of apoptosis and necrosis. Brain Res. Bull. *46*, 281–309.

Maryon, E.B., Coronado, R., and Anderson, P. (1996). *unc-68* encodes a ryanodine receptor involved in regulating *C. elegans* body-wall muscle contraction. J. Cell Biol. *134*, 885–893.

Matsuoka, K., Seta, K., Yamakawa, Y., Okuyama, T., Shinoda, T., and Isobe, T. (1994). Covalent structure of bovine brain calreticulin. Biochem. J. *298*, 435–442.

Mattson, M.P., LaFerla, F.M., Chan, S.L., Leissring, M.A., Shepel, P.N., and Geiger, J.D. (2000). Calcium signaling in the ER: its role in neuronal plasticity and neurodegenerative disorders. Trends Neurosci. *23*, 222–229.

Mello, C., and Fire, A. (1995). DNA transformation. Methods Cell Biol. *48*, 451–482.

Mesaeli, N., Nakamura, K., Zvaritch, E., Dickie, P., Dziak, E., Krause, K.H., Opas, M., MacLennan, D.H., and Michalak, M. (1999). Calreticulin is essential for cardiac development. J. Cell Biol. *144*, 857–868.

Metzstein, M.M., Stanfield, G.M., and Horvitz, H.R. (1998). Genetics of programmed cell death in *C. elegans*: past, present and future. Trends Genet. *14*, 410–416.

Michalak, M., Corbett, E.F., Mesaeli, N., Nakamura, K., and Opas, M. (1999). Calreticulin: one protein, one gene, many functions. Biochem. J. *344*, 281–292.

Mitani, S., Du, H., Hall, D.H., Driscoll, M., and Chalfie, M. (1993). Combinatorial control of touch receptor neuron expression in *Caenorhabditis elegans*. Development *119*, 773–783.

Mody, I., and MacDonald, J.F. (1995). NMDA receptor-dependent excitotoxicity: the role of intracellular Ca^{2+} release. Trends Pharmacol. Sci. *16*, 356–359.

Nagatomo, I., Hashiguchi, W., Tominaga, M., Akasaki, Y., Uchida, M., and Takigawa, M. (2001). Effects of MK-801, dantrolene, and FK506 on convulsive seizures and brain nitric oxide production in seizure-susceptible EL mice. Brain Res. *888*, 306–310.

Park, B.-J., Lee, D.-G., Yu, J.-R., Jung, S.-K., Choi, K., Lee, J.S., Lee, J.Y., Kim, Y.S., Lee, J.I., and Kwon, J.Y., Lee, J., Singson, A., Song, W.K., Eom, S.H., Park, C.-S., Kim, D.H., Bandyopadhyay, J., and Ahnn, J. (2001). Calreticulin, a calcium-binding molecular chaperone, is required for stress response and fertility in *C. elegans*. Mol. Biol. Cell *12*, 2835–2845.

Pozzan, T., Rizzuto, R., Volpe, P., and Meldolesi, J. (1994). Molecular and cellular physiology of intracellular calcium stores. Physiol. Rev. *74*, 595–636.

Rauch, F., Prud'homme, J., Arabian, A., Dedhar, S., and St-Arnaud, R. (2000). Heart, brain, and body wall defects in mice lacking calreticulin. Exp. Cell Res. *256*, 105–111.

Sattler, R., and Tymianski, M. (2000). Molecular mechanisms of calcium-dependent excitotoxicity. J. Mol. Med. *78*, 3–13.

Segal, M., and Manor, D. (1992). Confocal microscopic imaging of $[Ca^{2+}]i$ in cultured rat hippocampal neurons following exposure to N-methyl-D-aspartate. J. Physiol. *448*, 655–676.

Shreffler, W., Magardino, T., Shekdar, K., and Wolinsky, E. (1995). The unc-8 and sup-40 genes regulate ion channel function in *Caenorhabditis elegans* motorneurons. Genetics *139*, 1261–1272.

Smith, M.J. (1992). A *C. elegans* gene encodes a protein homologous to mammalian calreticulin. DNA Seq. *2*, 235–240.

Song, S.K., Karl, I.E., Ackerman, J.J., and Hotchkiss, R.S. (1993). Increased intracellular Ca^{2+}: a critical link in the pathophysiology of sepsis? Proc. Natl. Acad. Sci. USA *90*, 3933–3937.

Takemura, H., Hughes, A.R., Thastrup, O., and Putney, J.W., Jr. (1989). Activation of calcium entry by the tumor promoter thapsigargin in parotid acinar cells. Evidence that an intracellular calcium pool and not an inositol phosphate regulates calcium fluxes at the plasma membrane. J. Biol. Chem. *264*, 12266–12271.

Tavernarakis, N., Shreffler, W., Wang, S., and Driscoll, M. (1997). *unc-8*, a DEG/ENaC family member, encodes a subunit of a candidate mechanically gated channel that modulates *C. elegans* locomotion. Neuron *18*, 107–119.

Tavernarakis, N., Wang, S.L., Dorovkov, M., Ryazanov, A., and Driscoll, M. (2000). Heritable and inducible genetic interference by double-stranded RNA encoded by transgenes. Nat. Genet. *24*, 180–183.

Thomas, J.H. (1990). Genetic analysis of defecation in *Caenorhabditis elegans*. Genetics *124*, 855–872.

Treinin, M., and Chalfie, M. (1995). A mutated acetylcholine receptor subunit causes neuronal degeneration in *C. elegans*. Neuron *14*, 871–877.

Treinin, M., Gillo, B., Liebman, L., and Chalfie, M. (1998). Two functionally dependent acetylcholine subunits are encoded in a single *Caenorhabditis elegans* operon. Proc. Natl. Acad. Sci. USA *95*, 15492–15495.

Vassilakos, A., Michalak, M., Lehrman, M.A., and Williams, D.B. (1998). Oligosaccharide binding characteristics of the molecular chaperones calnexin and calreticulin. Biochemistry *37*, 3480–3490.

Waldmann, R., Champigny, G., Voilley, N., Lauritzen, I., and Lazdunski, M. (1996). The mammalian degenerin MDEG, an amiloride-sensitive cation channel activated by mutations causing neurodegeneration in *Caenorhabditis elegans*. J. Biol. Chem. *27*, 10433–10436.

Weber, J.T., Rzigalinski, B.A., Willoughby, K.A., Moore, S.F., and Ellis, E.F. (1999). Alterations in calcium-mediated signal transduction after traumatic injury of cortical neurons. Cell Calcium *26*, 289–299.

Williams, B.D., Schrank, B., Huynh, C., Shownkeen, R., and Waterston, R.H. (1992). A genetic mapping system in *Caenorhabditis elegans* based on polymorphic sequence-tagged sites. Genetics *131*, 609–624.

Zhang, L., Andou, Y., Masuda, S., Mitani, A., and Kataoka, K. (1993). Dantrolene protects against ischemic, delayed neuronal death in gerbil brain. Neurosci. Lett. *158*, 105–108.